Acta Mech 234, 3483–3498 (2023)
https://doi.org/10.1007/s00707-023-03571-w

ORIGINAL PAPER

Guoquan Nie · Jiapeng Zhuang · Jinxi Liu · Lele Zhang

Localized bending waves along the edge of a piezoelectric sandwich plate

Received: 26 December 2022 / Revised: 2 March 2023 / Accepted: 11 April 2023 / Published online: 27 April 2023

Abstract This paper deals with the propagation of bending waves along the free edge of a piezoelectric sandwich plate. The structure consists of a piezoelectric layer sandwiched between two metal layers. The first-order Zig-Zag approximation for in-plane displacements through the thickness of each layer is used. Interfacial continuity of the displacement and the transverse shear stress between the piezoelectric layer and the metal layer is ensured which is very important and also experienced by layered structures. The number of independent unknown variables is reduced from 14 to 4 by using the interfacial continuity and the zero shear stresses conditions at the top and bottom surfaces. The governing equations and corresponding boundary conditions are derived using Hamiltonian principle. The dispersion relations for electrically open and shorted boundary conditions imposed at the edge of the semi-infinite piezoelectric sandwich plate are obtained. The effects of electrical edge condition, layer thickness ratio and material property on dispersion characteristics of the localized bending waves are discussed. The numerical results show that the electrical edge condition has significant influence on dispersion property compared to edge wave in a piezoelectric single-layer plate. The phase velocity and the localization of bending edge wave significantly depend on the thickness of metal layer, and a thick metal layer can result in a high wave velocity and a strong localization. The phase velocity of bending wave is positively related to the velocities of classical Rayleigh surface wave in piezoelectric half-space and metal half-space under plane strain.

1 Introduction

An edge wave in a thin elastic plate is a traveling wave that propagates along the edge of the plate and decays exponentially with the distance from the edge. The existence of the flexural wave guided by the free edge of a semi-infinite isotropic elastic thin plate was first demonstrated by Konenkov in 1960 [1]. Theories related to the edge waves have attracted much attention in the last few decades due to its potential applications in the measurement of material properties and nondestructive evaluation of thin elastic structures, such as aircraft wings, submarine hulls, turbine or propeller blades, and so on [2]. It was demonstrated that a flexural wave localized along the free edge of a thin plate occurs only when Poisson's ratio is unequal to zero. This is because the free edge locally relieves the transverse stresses which are accompanied with a flexural wave. There are no transverse stresses to be relieved in the case of zero Poisson's ratio, and the localized flexural wave vanishes

G. Nie · J. Liu
State Key Laboratory of Mechanical Behavior and System Safety of Traffic Engineering Structures, Shijiazhuang Tiedao University, Shijiazhuang 050043, China

G. Nie
School of Mechanical Engineering, Shijiazhuang Tiedao University, Shijiazhuang 050043, China

J. Zhuang · L. Zhang (✉)
Department of Engineering Mechanics, Shijiazhuang Tiedao University, Shijiazhuang 050043, China
e-mail: zhangll@stdu.edu.cn

[3]. When waves localize along the edge of a thin elastic plate, complicated wave forms generate due to the interaction of Rayleigh–Lamb modes diffracted by either the edge, a defect close to the edge or both. This presents considerable challenges in identifying and interpreting these modes.

In view of the potential importance and applications, the existence and propagation of edge waves in various elastic structures have become an important research topic in the field of wave motion. Norris [4] proved that the edge wave also exists in the anisotropic plates using the classical theory of plate flexural. A unique wave solution was found on an orthotropic plate when the free edge is parallel to a principal direction of the material. Thompson and Abrahams [5] further studied edge wave propagating along non-principal directions of orthotropic plates. They also found that a unique solution of edge wave exists for arbitrary inclination angle. Zakharov and Becker [6] extended the studies to anisotropic media and presented some unique properties of Rayleigh type bending waves resulting from the anisotropic orientation. Fu [7] derived an explicit secular equation of the edge waves in a generally anisotropic elastic plate with a Stroh-like formalism and found that whenever an edge wave exists it must be unique. Liu et al. [8] proposed a semi-exact method to study the edge wave in semi-infinite isotropic plates, as well as anisotropic and anisotropic laminated plates. Fu and Brookes [9] demonstrated that a semi-infinite asymmetrical anisotropic thin plate can support at most two edge waves based on the Stroh-like formalism derived. Lu et al. [10] further extended the work by Fu and Brookes [9] to discuss and present the existence conditions for one or two subsonic edge waves propagating in such a plate. An efficient procedure for computing the explicit secular equation for the edge wave speed was proposed.

Most of the previous studies on the flexural edge wave in a semi-infinite thin elastic plate were derived from the classical Kirchhoff plate theory. Lagasse and Oliner [11] presented a comparative study on flexural edge wave including a finite element calculation and a measurement which were in good agreement with each other. It was shown that the thin plate results agree well with the finite element calculations and measured data in the low frequency limit, but for higher frequencies those results are no longer valid. Norris et al. [12] demonstrated that the essential characteristics of the flexural edge wave are also captured by the Mindlin plate theory. Their results agreed well with the measured data. Piliposian et al. [13] derived the dispersion equation of bending edge wave propagation in a transversely isotropic plate within the framework of the high-order refined theories of elastic plates. They found that there are no qualitative differences between the results obtained by the first-order Reissner–Mindlin plate theory and the high-order Ambartsumian plate theory. Relevant research progress includes bending edge wave in a semi-infinite thin plate with edge reinforced by a strip plate [14, 15] or a beam [16, 17], as well as a semi-infinite plate supported by a Winkler foundation [18–21] or a Pasternak foundation [22], and a semi-infinite plate immersed in a fluid [23]. Lawrie and Kaplunov [2] gave a periodic overview on edge waves and edge resonance in elastic structures before the 2010s. More recently, Kaplunov et al. [24] established a set of asymptotically justified boundary conditions for a semi-infinitely asymmetric sandwich strip with high-contrast properties under anti-plane shear using the Saint-Venant principle. Wilde et al. [25] constructed the asymptotically the refined boundary conditions for dynamics of plate bending. Two dynamics examples were considered to demonstrate that the derived refined boundary conditions extend the applicable range in 10 times comparing with that of the Kirchhoff theory.

Piezoelectric materials are widely used to develop electro-mechanical transducers for converting mechanical energy to electric energy or vice versa, and acoustic wave devices for frequency operation and sensing. Propagation of elastic wave in various piezoelectric materials and structures has received much interest due to its importance. From the existing literature, most studies dealt with the infinite piezoelectric media extended in one or two dimensions. As we know, a edge wave localizes near the edge of a thin elastic structures which means that there is nearly no resonances away from the active edge. This is very beneficial for mounting and supporting acoustic wave devices without interference to their operations. For edge waves in the semi-infinite piezoelectric structures, however, available theoretical results are very limited and most of them are for the single-layer plates. Piliposian and Ghazaryan [26] studied bending waves propagation along the free edge of a semi-infinite piezoelectric plate using Ambartsumian refined plate theory. The existence conditions were given. Recently, Althobaiti and Hawwa [21] considered bending edge waves propagating in a semi-infinite Kirchhoff piezoelectric plate supported by a Winkler–Fuss foundation. The dispersion relation was derived analytically. Our recent work showed that propagation of the bending edge wave can be multi-mode when a metal strip plate is bonded to the edge of a semi-infinite piezoelectric plate [15]. We further presented a comparative study on bending edge waves in a semi-infinite piezoelectric plate using three different plate theories [27]. We found that the dispersion curves predicted by the two-variable refined plate theory and the first-order Reissner–Mindlin plate theory have very small difference over the complete frequency range, but the results by the classical plate theory are much larger than the two theories.

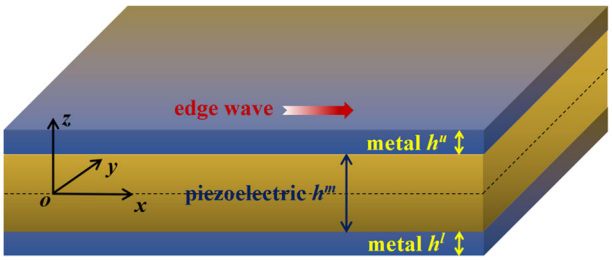

Fig. 1 Geometry of a semi-infinite piezoelectric sandwich plate

In this paper, we study the propagation of bending waves localized along the free edge of a semi-infinite piezoelectric sandwich plate. Zig-Zag theory of first-order approximation is used. The governing equations are derived using Hamiltonian principle. Our aim is to examine the effects of electrical edge condition, geometry and material property on dispersion characteristics of edge waves. To the best of our knowledge, the propagation of edge waves in a semi-infinite piezoelectric sandwich plate has not been previously considered and also has not been analyzed in the context of Zig-Zag theory.

2 Problem formulation and basic equations

Consider a semi-infinitely piezoelectric sandwich plate of total thickness H, as shown in Fig. 1. The structure consists of a transversely isotropic piezoelectric layer of thickness h^m sandwiched between a upper metal layer of thickness h^u and a lower metal layer of thickness h^l. The sandwich plate $(-\infty < x < \infty,\ 0 \le y < \infty,\ -H/2 \le z \le H/2)$ is referred to rectangular coordinates $(x,\ y,\ z)$ and is bounded by a free edge at $y = 0$. We consider bending wave propagating along the free edge of the semi-infinitely piezoelectric sandwich plate. A first-order Zig-Zag approximation theory [28–32] is used to model the considered piezoelectric sandwich plate. In each layer, the in-plane displacements are assumed to vary linearly along the thickness of the sandwich plate. The constant transverse displacement is assumed in the thickness direction, so that the transverse strain $\varepsilon_{zz} = 0$. Based on the above assumptions, the displacement of an arbitrary point along the x-axis, y-axis and z-axis, denoted as $u_x^k(x,\ y,\ z,\ t)$, $u_y^k(x,\ y,\ z,\ t)$ and $u_z^k(x,\ y,\ z,\ t)$, can be expressed as

$$\begin{cases} u_x^k(x,y,z,t) = U^k(x,y,t) + z\vartheta_x^k(x,y,t) \\ u_y^k(x,y,z,t) = V^k(x,y,t) + z\vartheta_y^k(x,y,t) \\ u_z^k(x,y,z,t) = W(x,y,t) \end{cases} \tag{1}$$

where the superscript $k = m, u$ and l, representing the middle piezoelectric layer, the upper metal layer and the lower metal layer, respectively. $U^k(x,\ y,\ t)$, $V^k(x,\ y,\ t)$ and $\vartheta_x^k(x,\ y,\ t)$, $\vartheta_y^k(x,\ y,\ t)$ denote displacement and rotation variables of the corresponding k layer. $W(x,y,t)$ is the transverse displacement of the sandwich plate.

For the piezoelectric sandwich plate under consideration, it is assumed that the middle piezoelectric layer, the upper and lower metal layers (can be regarded as two electrodes) are all very thin and are of comparable thickness. In this case, the two metal electrodes should be, respectively, modeled as two layers with finite thickness, not the thin electrodes with negligible mechanical effects treated in most of the literature. The two electrodes may be made of different materials or with different thicknesses. Due to the relatively thick metal layers, the electric field distributes in the middle piezoelectric layer only, not through the entire thickness of sandwich plate. As a result, the distribution of the electric field in the middle piezoelectric layer must satisfy the Maxwell equation. The electric potential φ^m is approximately assumed as a combination of a half-cosine and linear variation [33]

$$\varphi^m(x,y,z,t) = -\cos(\beta z)\Phi(x,y,t) + \frac{2zV_0}{h^m} \tag{2}$$

where $\beta = \pi/h^m$. V_0 is the value of the external electric voltage along z-direction. $\Phi(x,\ y,\ t)$ is the spatial and time variation of the electric potential in the mid-plane of the piezoelectric layer. Since only wave propagation analysis is addressed in this paper, the linear term in Eq. (2) can be ignored, i.e., $V_0 = 0$ [33].

The strain–displacement relations of the sandwich plate are

$$\begin{cases} \varepsilon_{xx}^k = \dfrac{\partial U^k}{\partial x} + z\dfrac{\partial \vartheta_x^k}{\partial x},\ \varepsilon_{yy}^k = \dfrac{\partial V^k}{\partial y} + z\dfrac{\partial \vartheta_y^k}{\partial y}, \\ \varepsilon_{yz}^k = \dfrac{1}{2}\left(\vartheta_y^k + \dfrac{\partial W}{\partial y}\right),\ \varepsilon_{xz}^k = \dfrac{1}{2}\left(\vartheta_x^k + \dfrac{\partial W}{\partial x}\right), \\ \varepsilon_{xy}^k = \dfrac{1}{2}\left(\dfrac{\partial U^k}{\partial y} + \dfrac{\partial V^k}{\partial x}\right) + \dfrac{z}{2}\left(\dfrac{\partial \vartheta_y^k}{\partial x} + \dfrac{\partial \vartheta_x^k}{\partial y}\right) \end{cases} \tag{3}$$

The constitutive relations for a transversely isotropic piezoelectric layer with z-axis being the crystallographic axis of symmetry are given by [15]

$$\begin{Bmatrix} \sigma_{xx}^m \\ \sigma_{yy}^m \\ \sigma_{zz}^m \\ \sigma_{yz}^m \\ \sigma_{xz}^m \\ \sigma_{xy}^m \end{Bmatrix} = \begin{bmatrix} c_{11} & c_{12} & c_{13} & 0 & 0 & 0 \\ & c_{11} & c_{13} & 0 & 0 & 0 \\ & & c_{33} & 0 & 0 & 0 \\ & & & c_{44} & 0 & 0 \\ & \text{sym.} & & & c_{44} & 0 \\ & & & & & c_{66} \end{bmatrix} \begin{Bmatrix} \varepsilon_{xx}^m \\ \varepsilon_{yy}^m \\ \varepsilon_{zz}^m \\ 2\varepsilon_{yz}^m \\ 2\varepsilon_{xz}^m \\ 2\varepsilon_{xy}^m \end{Bmatrix} - \begin{bmatrix} 0 & 0 & e_{31} \\ 0 & 0 & e_{31} \\ 0 & 0 & e_{33} \\ 0 & e_{15} & 0 \\ e_{15} & 0 & 0 \\ 0 & 0 & 0 \end{bmatrix} \begin{Bmatrix} E_x^m \\ E_y^m \\ E_z^m \end{Bmatrix} \tag{4}$$

$$\begin{Bmatrix} D_x^m \\ D_y^m \\ D_z^m \end{Bmatrix} = \begin{bmatrix} 0 & 0 & 0 & 0 & e_{15} & 0 \\ 0 & 0 & 0 & e_{15} & 0 & 0 \\ e_{31} & e_{31} & e_{33} & 0 & 0 & 0 \end{bmatrix} \begin{Bmatrix} \varepsilon_{xx}^m \\ \varepsilon_{yy}^m \\ \varepsilon_{zz}^m \\ 2\varepsilon_{yz}^m \\ 2\varepsilon_{xz}^m \\ 2\varepsilon_{xy}^m \end{Bmatrix} + \begin{bmatrix} s_{11} & 0 & 0 \\ 0 & s_{11} & 0 \\ 0 & 0 & s_{33} \end{bmatrix} \begin{Bmatrix} E_x^m \\ E_y^m \\ E_z^m \end{Bmatrix} \tag{5}$$

where σ^m and ε^m are the stress and strain of piezoelectric layer, D^m and E^m are the electric displacement and electric field, respectively. c, e and s are the elastic stiffness constant, piezoelectric constant and dielectric constant, respectively, and $c_{66} = (c_{11} - c_{12})/2$.

Using Eq. (2), the electric fields of the middle piezoelectric layer can be expressed as

$$\begin{cases} E_x^m = \cos(\beta z)\dfrac{\partial \Phi}{\partial x},\ E_y^m = \cos(\beta z)\dfrac{\partial \Phi}{\partial y}, \\ E_z^m = -\beta \sin(\beta z)\Phi \end{cases} \tag{6}$$

Then, the transverse shear stresses of the middle piezoelectric layer σ_{yz}^m and σ_{xz}^m are

$$\begin{cases} \sigma_{yz}^m = c_{44}\left(\vartheta_y^m + \dfrac{\partial W}{\partial y}\right) - e_{15}\left[\cos(\beta z)\dfrac{\partial \Phi}{\partial y}\right] \\ \sigma_{xz}^m = c_{44}\left(\vartheta_x^m + \dfrac{\partial W}{\partial x}\right) - e_{15}\left[\cos(\beta z)\dfrac{\partial \Phi}{\partial x}\right] \end{cases} \tag{7}$$

Similarly, transverse shear stresses of the upper and lower metal layers are

$$\begin{cases} \sigma_{yz}^{u,l} = \mu^{u,l}\left(\vartheta_y^{u,l} + \dfrac{\partial W}{\partial y}\right) \\ \sigma_{xz}^{u,l} = \mu^{u,l}\left(\vartheta_x^{u,l} + \dfrac{\partial W}{\partial x}\right) \end{cases} \tag{8}$$

where μ^u and μ^l are the shear modulus of the upper and lower metal layers, respectively.

Then, the unknown functions U^k, V^k, ϑ_x^k and ϑ_y^k are determined using the interface continuity and the traction-free conditions. At the top and bottom surfaces of the sandwich plate $\left(z = h^u + h^m/2 \quad \text{and} \quad z = -h^l - h^m/2\right)$, the traction-free condition requires:

$$\vartheta_x^l = \vartheta_x^u = -\frac{\partial W}{\partial x},\ \vartheta_y^l = \vartheta_y^u = -\frac{\partial W}{\partial y} \tag{9}$$

The transverse shear stresses are continuous at the interfaces $z = \pm h^m/2$, i.e., $\sigma_{xz}^l = \sigma_{xz}^m,\ \sigma_{yz}^l = \sigma_{yz}^m$. Using Eqs. (7) and (8) obtains:

$$\vartheta_x^m = -\frac{\partial W}{\partial x},\ \vartheta_y^m = -\frac{\partial W}{\partial y} \tag{10}$$

The in-plane displacements are also continuous at the interfaces $z = \pm h^m/2$, that is, $u_x^l = u_x^m,\ u_y^l = u_y^m$. With the aid of Eqs. (9) and (10), we give the following relations:

$$U^l = U^u = U^m, V^l = V^u = V^m \tag{11}$$

Letting $U^k(x,\ y,\ t) = U(x,\ y,\ t)$ and $V^k(x,\ y,\ t) = V(x,\ y,\ t)$, and taking account of the above relations, we rewrite the strain–displacement relation in the form:

$$\begin{cases} \varepsilon_{xx}^k = \dfrac{\partial U}{\partial x} - z\dfrac{\partial^2 W}{\partial x^2},\ \varepsilon_{yy}^k = \dfrac{\partial V}{\partial y} - z\dfrac{\partial^2 W}{\partial y^2}, \\ \varepsilon_{xy}^k = \dfrac{1}{2}\left(\dfrac{\partial U}{\partial y} + \dfrac{\partial V}{\partial x}\right) - z\dfrac{\partial^2 W}{\partial x \partial y} \end{cases} \tag{12}$$

3 Governing equations and boundary conditions

The total strain energy Π_S of the piezoelectric sandwich plate is given by [34]

$$\begin{aligned} \Pi_S = & \frac{1}{2}\int_A \int_{-h^l - h^m/2}^{-h^m/2} \left(\sigma_{xx}^l \varepsilon_{xx}^l + \sigma_{yy}^l \varepsilon_{yy}^l + 2\sigma_{xy}^l \varepsilon_{xy}^l\right) \mathrm{d}z\mathrm{d}A \\ & + \frac{1}{2}\int_A \int_{h^m/2}^{h^u + h^m/2} \left(\sigma_{xx}^u \varepsilon_{xx}^u + \sigma_{yy}^u \varepsilon_{yy}^u + 2\sigma_{xy}^u \varepsilon_{xy}^u\right) \mathrm{d}z\mathrm{d}A \\ & + \frac{1}{2}\int_A \int_{-h^m/2}^{h^m/2} \left(\sigma_{xx}^m \varepsilon_{xx}^m + \sigma_{yy}^m \varepsilon_{yy}^m + 2\sigma_{xy}^m \varepsilon_{xy}^m\right) \mathrm{d}z\mathrm{d}A \\ & - \frac{1}{2}\int_A \int_{-h^m/2}^{h^m/2} \left(D_x^m E_x^m + D_y^m E_y^m + D_z^m E_z^m\right) \mathrm{d}z\mathrm{d}A \end{aligned} \tag{13}$$

where A denotes the domain occupied by the mid-plane of each layer. Substituting Eqs. (6) and (12) into Eq. (13) yields

$$\begin{aligned} \Pi_S = & \frac{1}{2}\int_A \left(N_x \frac{\partial U}{\partial x} + N_y \frac{\partial V}{\partial y} + N_{xy} \frac{\partial U}{\partial y} + N_{xy} \frac{\partial V}{\partial x}\right) \mathrm{d}A \\ & - \frac{1}{2}\int_A \left(M_x \frac{\partial^2 W}{\partial x^2} + M_y \frac{\partial^2 W}{\partial y^2} + 2M_{xy} \frac{\partial^2 W}{\partial x \partial y}\right) \mathrm{d}A \\ & - \frac{1}{2}\int_A \int_{-h^m/2}^{h^m/2} \left\{D_x^m \cos(\beta z) \frac{\partial \Phi}{\partial x} + D_y^m \cos(\beta z) \frac{\partial \Phi}{\partial y} + D_z^m \beta \sin(\beta z) \Phi\right\} \mathrm{d}z\mathrm{d}A \end{aligned} \tag{14}$$

where $N_x = N_x^l + N_x^u + N_x^m$, $N_y = N_y^l + N_y^u + N_y^m$, $N_{xy} = N_{xy}^l + N_{xy}^u + N_{xy}^m$, $M_x = M_x^l + M_x^u + M_x^m$, $M_y = M_y^l + M_y^u + M_y^m$, $M_{xy} = M_{xy}^l + M_{xy}^u + M_{xy}^m$. N_x^k, N_y^k and N_{xy}^k are the axial forces and shearing force; M_x^k, M_y^k and M_{xy}^k are the bending moments and twisting moment, respectively. The expressions of these parameters can be found in Appendix A.

The kinetic energy Π_K of the piezoelectric sandwich plate is calculated by

$$\begin{aligned}\Pi_K &= \frac{1}{2}\rho^l \int_A \int_{-h^l-h^m/2}^{-h^m/2} \left[\left(\frac{\partial u_x^l}{\partial t}\right)^2 + \left(\frac{\partial u_y^l}{\partial t}\right)^2 + \left(\frac{\partial u_z^l}{\partial t}\right)^2\right] \mathrm{d}z\mathrm{d}A \\ &\quad + \frac{1}{2}\rho^u \int_A \int_{h^m/2}^{h^u+h^m/2} \left[\left(\frac{\partial u_x^u}{\partial t}\right)^2 + \left(\frac{\partial u_y^u}{\partial t}\right)^2 + \left(\frac{\partial u_z^u}{\partial t}\right)^2\right] \mathrm{d}z\mathrm{d}A \\ &\quad + \frac{1}{2}\rho^m \int_A \int_{-h^m/2}^{h^m/2} \left[\left(\frac{\partial u_x^m}{\partial t}\right)^2 + \left(\frac{\partial u_y^m}{\partial t}\right)^2 + \left(\frac{\partial u_z^m}{\partial t}\right)^2\right] \mathrm{d}z\mathrm{d}A \\ &= \frac{1}{2}\int_A I_1 \left[\left(\frac{\partial U}{\partial t}\right)^2 + \left(\frac{\partial V}{\partial t}\right)^2 + \left(\frac{\partial W}{\partial t}\right)^2\right] \mathrm{d}A \\ &\quad + \frac{1}{2}\int_A 2I_2 \left(\frac{\partial U}{\partial t}\frac{\partial^2 W}{\partial x \partial t} + \frac{\partial V}{\partial t}\frac{\partial^2 W}{\partial y \partial t}\right) \mathrm{d}A + \frac{1}{2}\int_A I_3 \left[\left(\frac{\partial^2 W}{\partial x \partial t}\right)^2 + \left(\frac{\partial^2 W}{\partial y \partial t}\right)^2\right] \mathrm{d}A \end{aligned} \tag{15}$$

where the inertial coefficients $I_1 = I_1^l + I_1^u + I_1^m$, $I_2 = I_2^l + I_2^u + I_2^m$, $I_3 = I_3^l + I_3^u + I_3^m$, and I_1^k, I_2^k, I_3^k are given by

$$\begin{cases} I_1^k = \rho^k h^k,\ I_2^u = \dfrac{h^u + h^m}{2}\rho^u h^u,\ I_2^l = -\dfrac{h^l + h^m}{2}\rho^l h^l,\ I_2^m = 0, \\ I_3^u = \dfrac{3h^{m2} + 6h^m h^u + 4h^{u2}}{12}\rho^u h^u,\ I_3^l = \dfrac{3h^{m2} + 6h^m h^l + 4h^{l2}}{12}\rho^l h^l,\ I_3^m = \dfrac{\rho^m h^{m3}}{12} \end{cases} \tag{16}$$

where ρ^u, ρ^l and ρ^m are mass density of the piezoelectric layer, the upper metal layer and the lower metal layer, respectively. For the general case of $\rho^u = \rho^l$ and $h^u = h^l$, the inertial coefficient I_2 is equal to zero.

The governing equations and corresponding boundary conditions can be derived by Hamilton principle [35]

$$\delta \int_{t_1}^{t_2} (\Pi_S - \Pi_K)\mathrm{d}t = 0 \tag{17}$$

Substituting Eqs. (14) and (15) into the above equation, letting the coefficients of δU, δV, δW and $\delta\Phi$ in Eq. (17) be zero, the governing equations can be obtained as

$$\delta U:\ \frac{\partial N_x}{\partial x} + \frac{\partial N_{xy}}{\partial y} = 2I_1\frac{\partial^2 U}{\partial t^2} - 2I_2\frac{\partial^3 W}{\partial x \partial t^2} \tag{18}$$

$$\delta V:\ \frac{\partial N_{xy}}{\partial x} + \frac{\partial N_y}{\partial y} = 2I_1\frac{\partial^2 V}{\partial t^2} - 2I_2\frac{\partial^3 W}{\partial y \partial t^2} \tag{19}$$

$$\begin{aligned}\delta W:\ \frac{\partial^2 M_x}{\partial x^2} + \frac{\partial^2 M_y}{\partial y^2} + \frac{\partial^2 M_{xy}}{\partial x \partial y} &= 2I_1\frac{\partial^2 W}{\partial t^2} + 2I_2\frac{\partial^2}{\partial t^2}\left(\frac{\partial U}{\partial x} + \frac{\partial V}{\partial y}\right) \\ &\quad - 2I_3\frac{\partial^2}{\partial t^2}\left(\frac{\partial^2 W}{\partial^2 x} + \frac{\partial^2 W}{\partial^2 y}\right)\end{aligned} \tag{20}$$

$$\delta\Phi:\ \int_{-h/2}^{h/2}\left[\frac{\partial D_x^m}{\partial x}\cos(\beta z) + \frac{\partial D_y^m}{\partial y}\cos(\beta z) - D_z^m \beta \sin(\beta z)\right]\mathrm{d}z = 0 \tag{21}$$

and the corresponding boundary conditions are

$$\begin{cases} N_x + N_{xy} = 0 \text{ or } U = 0 \\ N_{xy} + N_y = 0 \text{ or } V = 0 \\ \dfrac{\partial M_x}{\partial x} + \dfrac{\partial M_y}{\partial y} + \dfrac{\partial M_{xy}}{\partial x} + \dfrac{\partial M_{xy}}{\partial y} - 2I_2\left(\dfrac{\partial^2 U}{\partial t^2} + \dfrac{\partial^2 V}{\partial t^2}\right) \\ +2I_3\dfrac{\partial^2}{\partial t^2}\left(\dfrac{\partial W}{\partial x} + \dfrac{\partial W}{\partial y}\right) = 0 \text{ or } W = 0 \\ M_x - M_{xy} - N_{xe}W = 0 \text{ or } \dfrac{\partial W}{\partial x} = 0 \\ M_y - M_{xy} - N_{ye}W = 0 \text{ or } \dfrac{\partial W}{\partial y} = 0 \\ \displaystyle\int_{-h/2}^{h/2}\left[D_x^m \cos(\beta z) + D_y^m \cos(\beta z)\right]\mathrm{d}z = 0 \text{ or } \Phi = 0 \end{cases} \tag{22}$$

4 Solutions of localized bending waves

For bending wave propagating along x-direction, we seek the general solution satisfying the governing equations in the form:

$$\begin{cases} U(x,y,t) = A\exp[-\mathrm{i}pky - \mathrm{i}k(x-ct)] \\ V(x,y,t) = B\exp[-\mathrm{i}pky - \mathrm{i}k(x-ct)] \\ W(x,y,t) = \mathrm{i}C\exp[-\mathrm{i}pky - \mathrm{i}k(x-ct)] \\ \Phi(x,y,t) = \mathrm{i}D\exp[-\mathrm{i}pky - \mathrm{i}k(x-ct)] \end{cases} \tag{23}$$

where $\mathrm{i} = \sqrt{-1}$, c is the phase velocity, k is the wavenumber, p is a parameter to be determined. A, B, C and D are unknown amplitudes. Substituting Eq. (23) into Eqs. (18)–(21) obtains:

$$\mathbf{Q}\cdot\mathrm{X} = \begin{bmatrix} Q_{11} & Q_{12} & Q_{13} & Q_{14} \\ Q_{21} & Q_{22} & Q_{23} & Q_{24} \\ Q_{31} & Q_{32} & Q_{33} & Q_{34} \\ Q_{41} & Q_{42} & Q_{43} & Q_{44} \end{bmatrix}\begin{pmatrix} A \\ B \\ C \\ D \end{pmatrix} = 0 \tag{24}$$

where $\mathbf{X} = [A,\ B,\ C,\ D]^{\mathrm{T}}$ is the unknown wave amplitude, and the elements of matrix $\mathbf{Q}$ are given in Appendix B. The non-trivial solution for the wave amplitude $\mathbf{X}$ requires the determinant of $\mathbf{Q}$ be zero, which yields ten roots of p representing the propagation direction of the ten partial waves, respectively. In order to satisfy the attenuation condition that the mechanical displacements and electrical potential should vanish as $y \to \infty$, only five roots having a negative imaginary part, denoted by p_j (j = 1–5), should be retained. The general solution to the governing equations can be written as:

$$\begin{cases} U(x,y,t) = \displaystyle\sum_{j=1}^{5}\alpha_j D_j \exp\left[-\mathrm{i}p_j ky - \mathrm{i}k(x-ct)\right] \\ V(x,y,t) = \displaystyle\sum_{j=1}^{5}\beta_j D_j \exp\left[-\mathrm{i}p_j ky - \mathrm{i}k(x-ct)\right] \\ W(x,y,t) = \displaystyle\sum_{j=1}^{5}\mathrm{i}\gamma_j D_j \exp\left[-\mathrm{i}p_j ky - \mathrm{i}k(x-ct)\right] \\ \Phi(x,y,t) = \displaystyle\sum_{j=1}^{5}\mathrm{i}D_j \exp\left[-\mathrm{i}p_j ky - \mathrm{i}k(x-ct)\right] \end{cases} \tag{25}$$

where $\alpha_j = A_j/D_j$, $\beta_j = B_j/D_j$ and $\gamma_j = C_j/D_j$ are amplitude ratios given by

$$\alpha_j = \frac{\begin{vmatrix} -Q_{14} & Q_{12} & Q_{13} \\ -Q_{24} & Q_{22} & Q_{23} \\ -Q_{34} & Q_{32} & Q_{33} \end{vmatrix}}{\begin{vmatrix} Q_{11} & Q_{12} & Q_{13} \\ Q_{21} & Q_{22} & Q_{23} \\ Q_{31} & Q_{32} & Q_{33} \end{vmatrix}}, \beta_j = \frac{\begin{vmatrix} Q_{11} & -Q_{14} & Q_{13} \\ Q_{21} & -Q_{24} & Q_{23} \\ Q_{31} & -Q_{34} & Q_{33} \end{vmatrix}}{\begin{vmatrix} Q_{11} & Q_{12} & Q_{13} \\ Q_{21} & Q_{22} & Q_{23} \\ Q_{31} & Q_{32} & Q_{33} \end{vmatrix}}, \gamma_j = \frac{\begin{vmatrix} Q_{11} & Q_{12} & -Q_{14} \\ Q_{21} & Q_{22} & -Q_{24} \\ Q_{31} & Q_{32} & -Q_{34} \end{vmatrix}}{\begin{vmatrix} Q_{11} & Q_{12} & Q_{13} \\ Q_{21} & Q_{22} & Q_{23} \\ Q_{31} & Q_{32} & Q_{33} \end{vmatrix}} \tag{26}$$

The boundary conditions at the free edge $y = 0$ are imposed in such a way that the axial force, the shearing force, the bending moment and the twisting moment are set to zero, i.e., $N_y = N_{xy} = M_y = M_{xy}$. For the piezoelectric layer, we further consider two types of electrical boundary conditions at the edge $y = 0$, i.e., $\int_{-h^m/2}^{h^m/2} D_y^m \mathrm{d}z = 0$ for electrically open case, and $\int_{-h^m/2}^{h^m/2} \varphi^m \mathrm{d}z = 0$ for electrically shorted case. Substituting the general solution (25) into the expresses of force and moment resultants given in Appendix A and then, into the above mechanical and electrical boundary conditions for free edge, a system of 5-order linear homogeneous equations with unknown amplitudes D_j yields, i.e., $\mathbf{T} \cdot \mathbf{D} = 0$, where $\mathbf{D} = [D_1,\ D_2,\ D_3,\ D_4,\ D_5]^{\mathrm{T}}$. The nonzero elements of the matrix $\mathbf{T}$ for electrically open case at the free edge are given by

$$\begin{aligned}
T_{1j} &= c_{12} + p_j\alpha_j n^l\left(\lambda^l + 2\mu^l\right) + p_j\alpha_j n^u\left(\lambda^u + 2\mu^u\right) + p_j\alpha_j c_{11} \\
&\quad + p_j^2\xi\beta_j\left(\lambda^l + 2\mu^l\right)n^l\left(n^l + 1\right)/2 - p_j^2\xi\beta_j\left(\lambda^u + 2\mu^u\right)n^u\left(n^u + 1\right)/2, \\
T_{2j} &= \left(p_j + \alpha_j\right)\left(n^l\mu^l + n^u\mu^u + c_{66}\right) + p_j\xi\beta_j n^l\left(n^l + 1\right)\mu^l - p_j\xi\beta_j n^u(n^u + 1)\mu^u, \\
T_{3j} &= -p_j\xi\alpha_j\left(\lambda^l + 2\mu^l\right)n^l\left(n^l + 1\right)/2 + p_j\xi\alpha_j\left(\lambda^u + 2\mu^u\right)n^u\left(n^u + 1\right)/2 \\
&\quad - p_j^2\xi^2\beta_j\left(\lambda^l + 2\mu^l\right)\left(3n^l + 6n^{l2} + 4n^{l3}\right)/12, \\
&\quad - p_j^2\xi^2\beta_j\left(\lambda^u + 2\mu^u\right)\left(3n^u + 6n^{u2} + 4n^{u3}\right)/12 - p_j^2\xi^2\beta_j(c_{11} + c_{12})/12 - 2e_{31}\gamma_j/\pi \\
T_{4j} &= -\xi\mu^l\left(p_j + \alpha_j\right)n^l\left(n^l + 1\right)/2 + \xi\mu^u\left(p_j + \alpha_j\right)n^u\left(n^u + 1\right)/2 \\
&\quad - p_j\xi^2\beta_j\mu^l\left(3n^l + 6n^{l2} + 4n^{l3}\right)/12 - p_j\xi^2\beta_j\mu^u\left(3n^u + 6n^{u2} + 4n^{u3}\right)/12 - p_j\xi^2\beta_j\frac{c_{66}}{6},
\end{aligned}$$

$T_{5j} = \xi\frac{2s_{11}p_j}{\pi}\gamma_j$.where $\xi = kh^m$ is the non-dimensional wavenumber. $n^u = h^u/h^m$ and $n^l = h^l/h^m$ are the thickness ratios of the upper and lower metal layers to the piezoelectric layer, respectively. The elements of matrix $\mathbf{T}$ for electrically shorted case are the same except for $T_{5j} = 2\gamma_j/\pi$. When the determinant of the matrix $\mathbf{T}$ vanishes, we obtain the dispersion relation for localized bending waves propagating in the considered piezoelectric sandwich plate.

5 Numerical results and discussions

In this section, some numerical results are provided to demonstrate the dispersion characteristics of localized bending waves propagating along the free edge of a metal/piezoelectric/metal sandwich plate. Unless otherwise specified, the piezoelectric layer is considered as PZT-4, the metal layers are copper, and the thickness ratios $n^u = n^l = n$. Their material constants can be found in Table 1 [36] and Table 2 [37].

To demonstrate the influence of electrical edge condition on wave dispersion, Fig. 2 shows the dispersion curves of localized bending wave along the edge of a copper/PZT-4/copper piezoelectric sandwich plate under electrically open and shorted edge conditions, where the thickness ratio $n = 0.1$. It is found that the electrical edge condition has very small impact on dispersion curve at the relative low non-dimensional wavenumber ξ (nearly no effect within the range $0 < \xi < 0.1$). This means that the effect of electrical condition imposed at the free edge can be ignored when the thickness of the sandwich plate is very thin, or the wavenumber is relatively low. The difference in phase velocity between electrically open case and shorted case becomes more significant as increasing ξ. It is clear that the phase velocity of electrically open case is higher than that of electrically shorted case.

To deeply understand the dispersion characteristics of edge wave in a piezoelectric sandwich plate, we use our previous results [15, 27] to calculate the edge wave velocity for a single-layer PZT-4 piezoelectric thin pate.

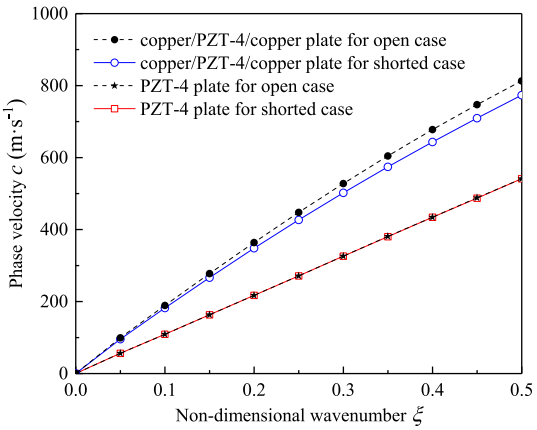

Fig. 2 Dispersion curves of localized bending wave under different electrical boundary conditions at the edge. Solid dots and open circles represent copper/PZT-4/copper sandwich plate under electrically open and shorted edge conditions, respectively; Asterisks and squares represent PZT-4 single-layer plate under electrically open and shorted edge conditions, respectively

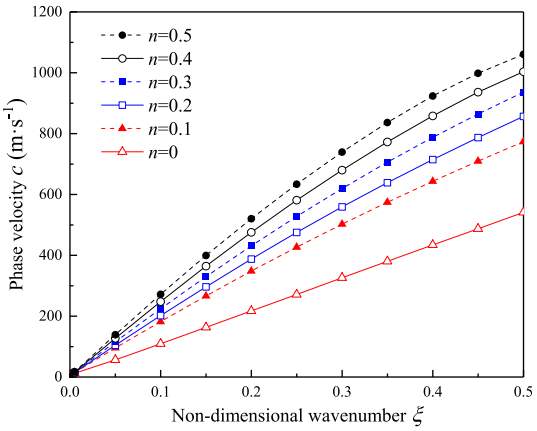

Fig. 3 Effect of thickness ratio on dispersion curves for electrically shorted case at the edge. Solid dots, open circles, solid squares, open squares, solid triangles and open triangles represent the case of thickness ratio $n = 0.5$, 0.4, 0.3, 0.2, 0.1 and 0, respectively

The obtained results agree very well with the present piezoelectric sandwich plate in the case of $n = 0$ which verify the validity of the present results. The dispersion curves of a PZT-4 single-layer pate are also plotted in Fig. 2 for comparison. It is found that the difference in phase velocity of the PZT-4 single-layer pate between electrically open case and shorted case is very undistinguished compared to that of the copper/PZT-4/copper sandwich plate. Moreover, the phase velocity of edge wave in PZT-4 single-layer plate is much lower than that of copper/PZT-4/copper sandwich plate. This demonstrates that the edge wave velocity is lowered when the surface electrodes are considered as the metal layers of finite thickness. At the same time, the change of wave velocity resulted from electrical condition imposed at the edge also becomes more significant. In the following examples, our discussions are focused on the case of electrically shorted condition at the edge.

To clearly show the effect of thickness of the metal layers on the dispersion property, Fig. 3 presents the dispersion curves of bending edge waves in copper/PZT-4/copper sandwich plate for selected thickness ratios. In this calculation, the thickness of PZT-4 layer is fixed, while the thicknesses of the upper and lower copper layers are the same and are taken as $0.1h^m$, $0.2h^m$ $0.3h^m$, $0.4h^m$ and $0.5h^m$, respectively. It is shown that the wave velocity significantly depends on the thickness of the metal layers. The larger the thickness of the metal layers, the higher the phase velocity of bending edge waves for a given non-dimensional wavenumber ξ. The wave velocity for the case of $n = 0$ is much lower than other cases as expected.

Localization of edge waves is an important performance reflecting the extent to which the vibration energy is confined to the edge region of a plate. The lowest absolute value of imaginary part of the five attenuation coefficients p_j ($j = 1$–5), denoted by η, is used to characterizing the localization of edge waves [13]. Figure 4 gives the effect of the thickness ratio on the localization coefficient η. It is shown that η monotonically increases

Table 1 Material constants of piezoelectric layer [34]

Piezoelectric	Elastic constants (10^9 N m^{-2})					Piezoelectric constants (C m^{-2})			Relative dielectric constants		Density (kg m^{-3})	Rayleigh surface wave velocity (m s^{-1})
	c_{11}	c_{12}	c_{13}	c_{33}	c_{44}	e_{31}	e_{33}	e_{15}	s_{33}/s_0	s_{11}/s_0	ρ	c_R
$BaTiO_3$	150	66	66	146	44	− 4.35	17.5	11.4	111.56	98.72	5700	2777.94
PZT-4	139	77.8	74.3	113	25.6	− 6.98	13.8	13.4	54.7	60.0	7500	2192.34
PZT-5H	126	79.5	84.1	117	23	− 6.5	23.3	17	14.7	17.0	7500	1980.94

where $s_0 = 8.854 \times 10^{-12}$ F m^{-1} is the dielectric constant of vacuum

Table 2 Material constants of metal layer [35]

Metal	Young's modulus (10^9 N m^{-2}) E	Shear modulus (10^9 N m-2) μ	Poisson ratio N	Density (kg m^{-3}) ρ	Rayleigh surface wave velocity (m s^{-1}) c_R
Steel	210	82.03	0.28	7800	2998.7
Copper	119	44.87	0.326	8900	2091.5
Silver	62.3	22.8	0.366	10,500	1380.7

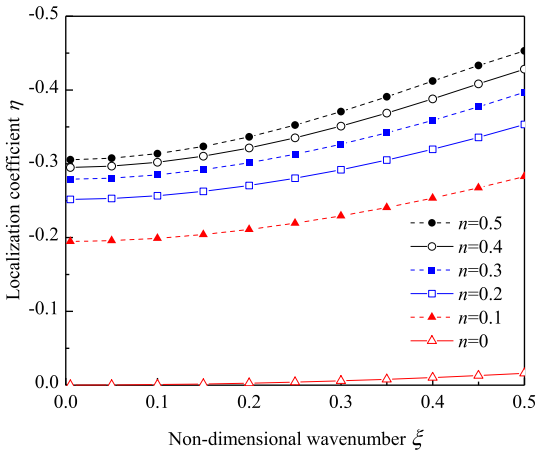

Fig. 4 Effect of thickness ratio on attenuation coefficient. Solid dots, open circles, solid squares, open squares, solid triangles and open triangles represent the case of thickness ratio $n = 0.5, 0.4, 0.3, 0.2, 0.1$ and 0, respectively

with increasing ξ. The localization of edge waves of a piezoelectric single plate (the case of $n = 0$) is much weaker than that of piezoelectric sandwich plate which means that when a bending edge wave propagating in a piezoelectric single plate, it decays slower from the free edge compared with a piezoelectric sandwich plate. The localization of edge waves of piezoelectric sandwich plate strongly depends on its thickness ratio. The larger the thickness of the metal layers, the stronger the localization of edge waves for a given ξ. This means that the bending edge wave is attenuating faster from the free edge of a piezoelectric sandwich plate with thick metal layers.

To reveal the effect of piezoelectric material property on dispersion characteristics of bending edge wave, we calculate the dispersion curves of three sandwich plates having different piezoelectric layer combined with copper layers, i.e., copper/$BaTiO_3$/copper, copper/PZT-4/copper and copper/PZT-5H/copper, which are shown in Fig. 5. The used materials constants can be found in Table 1. As we know, the propagation of edge waves in a semi-infinite isotropic elastic plate is the analogue of the classical Rayleigh surface wave in a traction-free half-space under plane strain. We thus calculate the Rayleigh surface wave velocities c_R of the considered three piezoelectric materials under electrically shorted surface condition, also listed in Table 1, which are 2777.94 m/s for $BaTiO_3$, 2192.34 m/s for PZT-4, and 1980.94 m/s for PZT-5H. Combined Fig. 4 and the above Rayleigh surface wave velocities, it is found that the phase velocity of bending edge wave is positively related to that of classical Rayleigh surface wave of piezoelectric layer. The larger the Rayleigh surface wave velocity, the faster the localized bending wave propagation along the edge of the semi-infinite piezoelectric sandwich plate. Figure 6 gives the dependence of metal material property on dispersion curves. In our calculation, the upper and lower metal layers are the same and are taken as steel, copper and silver, respectively. Their material constants are found in Table 2. Similarly, we calculate the Rayleigh surface wave velocities c_R of three different metal half-spaces under plane strain, also listed in Table 2, which are 2998.7 m/s for steel, 2091.5 m/s for copper, and 1380.7 m/s for silver. As it is expected, a metal layer with high c_R can produce a high velocity of bending edge wave. From this, it is deduced that any constituent of a metal/piezoelectric/metal sandwich plate having high Rayleigh surface wave velocity contributes to produce a high velocity of bending edge wave.

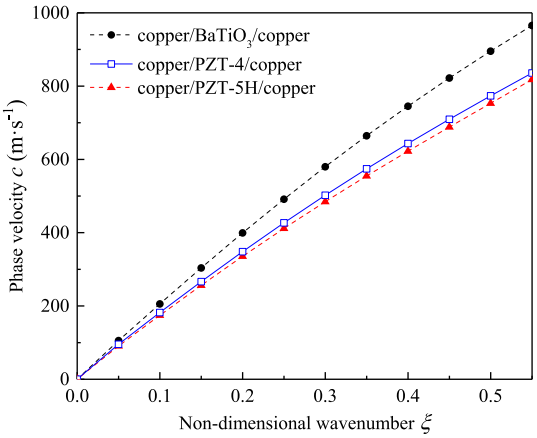

Fig. 5 Dispersion curves of bending wave with different piezoelectric materials for electrically shorted case at the edge. Solid dots, open squares and solid triangles represent the case that the middle piezoelectric layer materials are $BaTiO_3$, PZT-4 and PZT-5H, respectively

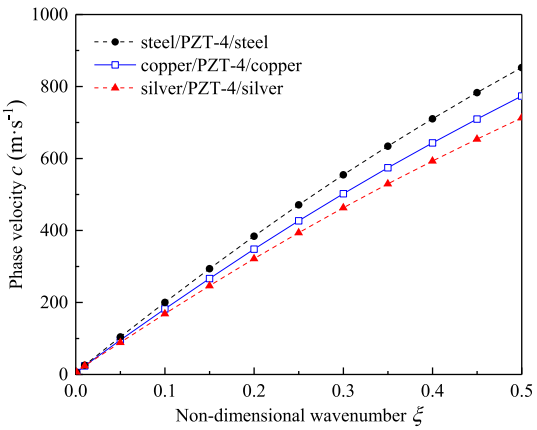

Fig. 6 Dispersion curves of bending wave with different metal materials for electrically shorted case at the edge. Solid dots, open squares and solid triangles represent the case that the upper and lower metal layers are steel, copper and silver, respectively

6 Conclusions

Propagation of localized bending waves along the free edge of a piezoelectric sandwich plate is investigated using the first-order Zig-Zag approximation theory. Interfacial continuity of the displacement and the transverse shear stress is ensured. The general solution satisfying the governing equations is obtained. Dispersion relation of localized bending waves is derived using the mechanical and electrical edge conditions. The effects of electrical edge conditions, thickness ratio and material property on the dispersion characteristics are discussed through the numerical examples. It is found that the electrical boundary condition imposed at the edge shows more significant influence on dispersion property of edge waves in a piezoelectric sandwich plate compared to such waves in a piezoelectric single-layer plate. The phase velocity of electrically open case is higher than that of electrically shorted case. The phase velocity and the localization of edge wave significantly depends on the thickness of metal layer. A large thickness of the metal layer results in a high wave velocity and a strong localization. The propagation velocity of bending edge wave in a piezoelectric sandwich plate is positively related to the classical Rayleigh surface wave velocities of piezoelectric half-space and metal half-space under plane strain.

Acknowledgements This study is supported by the National Natural Science Foundation of China (No. 11872041) and the Top-notch Young Talent Program of Hebei Province Education Department of China (No. BJK2022055).

Appendix A

Expressions of the axial forces, shearing force, bending moments and twisting moment in Eq. (14) are given by

$$\begin{cases} N_x^l = \int_{-h^l-h^m/2}^{-h^m/2} \left(\lambda^l+2\mu^l\right)\left(\dfrac{\partial U}{\partial x}-z\dfrac{\partial^2 W}{\partial x^2}\right)\mathrm{d}z = h^l\left(\lambda^l+2\mu^l\right)\left(\dfrac{\partial U}{\partial x}+\dfrac{h^l+h^m}{2}\dfrac{\partial^2 W}{\partial x^2}\right) \\ N_x^u = \int_{h^m/2}^{h^u+h^m/2} \left(\lambda^u+2\mu^u\right)\left(\dfrac{\partial U}{\partial x}-z\dfrac{\partial^2 W}{\partial x^2}\right)\mathrm{d}z = h^u\left(\lambda^u+2\mu^u\right)\left(\dfrac{\partial U}{\partial x}-\dfrac{h^u+h^m}{2}\dfrac{\partial^2 W}{\partial x^2}\right) \\ N_x^m = \int_{-h^m/2}^{h^m/2} c_{11}\left(\dfrac{\partial U}{\partial x}-z\dfrac{\partial^2 W}{\partial x^2}\right)+c_{12}\left(\dfrac{\partial V}{\partial y}-z\dfrac{\partial^2 W}{\partial y^2}\right)+e_{31}\beta\sin(\beta z)\Phi\mathrm{d}z = h^m\left(c_{11}\dfrac{\partial U}{\partial x}+c_{12}\dfrac{\partial V}{\partial y}\right) \end{cases}$$

$$\begin{cases} N_y^l = \int_{-h^l-h^m/2}^{-h^m/2} \left(\lambda^l+2\mu^l\right)\left(\dfrac{\partial V}{\partial y}-z\dfrac{\partial^2 W}{\partial y^2}\right)\mathrm{d}z = h^l\left(\lambda^l+2\mu^l\right)\left(\dfrac{\partial V}{\partial y}+\dfrac{h^l+h^m}{2}\dfrac{\partial^2 W}{\partial y^2}\right) \\ N_y^u = \int_{h^m/2}^{h^u+h^m/2} \left(\lambda^u+2\mu^u\right)\left(\dfrac{\partial V}{\partial y}-z\dfrac{\partial^2 W}{\partial y^2}\right)\mathrm{d}z = h^u\left(\lambda^u+2\mu^u\right)\left(\dfrac{\partial V}{\partial y}-\dfrac{h^u+h^m}{2}\dfrac{\partial^2 W}{\partial y^2}\right) \\ N_y^m = \int_{-h^m/2}^{h^m/2} c_{12}\left(\dfrac{\partial U}{\partial x}-z\dfrac{\partial^2 W}{\partial x^2}\right)+c_{11}\left(\dfrac{\partial V}{\partial y}-z\dfrac{\partial^2 W}{\partial y^2}\right)+e_{31}\beta\sin(\beta z)\Phi\mathrm{d}z = h^m\left(c_{12}\dfrac{\partial U}{\partial x}+c_{11}\dfrac{\partial V}{\partial y}\right) \end{cases}$$

$$\begin{cases} N_{xy}^l = \int_{-h^l-h^m/2}^{-h^m/2} \mu^l\left(\dfrac{\partial U}{\partial y}+\dfrac{\partial V}{\partial x}-2z\dfrac{\partial^2 W}{\partial x\partial y}\right)\mathrm{d}z = h^l\mu^l\left[\dfrac{\partial U}{\partial y}+\dfrac{\partial V}{\partial x}+\left(h^l+h^m\right)\dfrac{\partial^2 W}{\partial x\partial y}\right] \\ N_{xy}^u = \int_{h^m/2}^{h^u+h^m/2} \mu^u\left(\dfrac{\partial U}{\partial y}+\dfrac{\partial V}{\partial x}-2z\dfrac{\partial^2 W}{\partial x\partial y}\right)\mathrm{d}z = h^u\mu^u\left[\dfrac{\partial U}{\partial y}+\dfrac{\partial V}{\partial x}-\left(h^u+h^m\right)\dfrac{\partial^2 W}{\partial x\partial y}\right] \\ N_{xy}^m = \int_{-h^m/2}^{h^m/2} c_{66}\left(\dfrac{\partial U}{\partial y}+\dfrac{\partial V}{\partial x}-2z\dfrac{\partial^2 W}{\partial x\partial y}\right)\mathrm{d}z = h^m c_{66}\left(\dfrac{\partial U}{\partial y}+\dfrac{\partial V}{\partial x}\right) \end{cases}$$

$$\begin{cases} M_x^l = \int_{-h^l-h^m/2}^{-h^m/2} \left[z\left(\lambda^l+2\mu^l\right)\left(\dfrac{\partial U}{\partial x}-z\dfrac{\partial^2 W}{\partial x^2}\right)\right]\mathrm{d}z \\ \quad = -h^l\left(\lambda^l+2\mu^l\right)\left[\dfrac{h^l+h^m}{2}\dfrac{\partial U}{\partial x}+\dfrac{3h^{m2}+6h^m h^l+4h^{l2}}{12}\dfrac{\partial^2 W}{\partial x^2}\right] \\ M_x^u = \int_{h^m/2}^{h+h^m/2^u} \left[z\left(\lambda^u+2\mu^u\right)\left(\dfrac{\partial U}{\partial x}-z\dfrac{\partial^2 W}{\partial x^2}\right)\right]\mathrm{d}z \\ \quad = h^u\left(\lambda^u+2\mu^u\right)\left[\dfrac{h^u+h^m}{2}\dfrac{\partial U}{\partial x}-\dfrac{3h^{m2}+6h^m h^u+4h^{u2}}{12}\dfrac{\partial^2 W}{\partial x^2}\right] \\ M_x^m = \int_{-h^m/2}^{h^m/2} zc_{11}\left(\dfrac{\partial U}{\partial x}-z\dfrac{\partial^2 W}{\partial x^2}\right)+zc_{12}\left(\dfrac{\partial V}{\partial y}-z\dfrac{\partial^2 W}{\partial y^2}\right)+ze_{31}\beta\sin(\beta z)\Phi\mathrm{d}z \\ \quad = -\dfrac{h^{m3}}{12}\left(c_{11}\dfrac{\partial^2 W}{\partial x^2}+c_{12}\dfrac{\partial^2 W}{\partial y^2}\right)+\dfrac{2h^m e_{31}}{\pi}\Phi \end{cases}$$

$$
\begin{cases}
M_y^l = \int_{-h^l-h^m/2}^{-h^m/2} z\left(\lambda^l+2\mu^l\right)\left(\dfrac{\partial V}{\partial y}-z\dfrac{\partial^2 W}{\partial y^2}\right)\mathrm{d}z \\
\quad = -h^l\left(\lambda^l+2\mu^l\right)\left[\dfrac{h^l+h^m}{2}\dfrac{\partial V}{\partial y}+\dfrac{3h^{m2}+6h^m h^l+4h^{l2}}{12}\dfrac{\partial^2 W}{\partial y^2}\right] \\
M_y^u = \int_{h^m/2}^{h^u+h^m/2}\left[z\left(\lambda^u+2\mu^u\right)\left(\dfrac{\partial V}{\partial y}-z\dfrac{\partial^2 W}{\partial y^2}\right)\right]\mathrm{d}z \\
\quad = h^u\left(\lambda^u+2\mu^u\right)\left[\dfrac{h^u+h^m}{2}\dfrac{\partial V}{\partial y}-\dfrac{3h^{m2}+6h^m h^u+4h^{u2}}{12}\dfrac{\partial^2 W}{\partial y^2}\right] \\
M_y^m = \int_{-h^m/2}^{h^m/2} zc_{12}\left(\dfrac{\partial U}{\partial x}-z\dfrac{\partial^2 W}{\partial x^2}\right)+zc_{11}\left(\dfrac{\partial V}{\partial y}-z\dfrac{\partial^2 W}{\partial y^2}\right)+ze_{31}\beta\sin(\beta z)\Phi\mathrm{d}z \\
\quad = -\dfrac{h^{m3}}{12}\left(c_{12}\dfrac{\partial^2 W}{\partial x^2}+c_{11}\dfrac{\partial^2 W}{\partial y^2}\right)+\dfrac{2e_{31}h^m}{\pi}\Phi
\end{cases}
$$

$$
\begin{cases}
M_{xy}^l = \int_{-h^l-h^m/2}^{-h^m/2} z\mu^l\left(\dfrac{\partial U}{\partial y}+\dfrac{\partial V}{\partial x}-2z\dfrac{\partial^2 W}{\partial x\partial y}\right)\mathrm{d}z \\
\quad = -h^l\mu^l\left[\dfrac{h^l+h^m}{2}\left(\dfrac{\partial U}{\partial y}+\dfrac{\partial V}{\partial x}\right)+\dfrac{3h^{m2}+6h^m h^l+4h^{l2}}{12}\dfrac{\partial^2 W}{\partial x\partial y}\right] \\
M_{xy}^u = \int_{h^m/2}^{h^u+h^m/2} z\mu^u\left(\dfrac{\partial U}{\partial y}+\dfrac{\partial V}{\partial x}-2z\dfrac{\partial^2 W}{\partial x\partial y}\right)\mathrm{d}z \\
\quad = h^u\mu^u\left[\dfrac{h^u+h^m}{2}\left(\dfrac{\partial U}{\partial y}+\dfrac{\partial V}{\partial x}\right)-\dfrac{3h^{m2}+6h^m h^u+4h^{u2}}{12}\dfrac{\partial^2 W}{\partial x\partial y}\right] \\
M_{xy}^m = \int_{-h^m/2}^{h^m/2} zc_{66}\left(\dfrac{\partial U}{\partial y}+\dfrac{\partial V}{\partial x}-2z\dfrac{\partial^2 W}{\partial x\partial y}\right)\mathrm{d}z = -\dfrac{c_{66}h^{m3}}{6}\dfrac{\partial^2 W}{\partial x\partial y}
\end{cases}
$$

where λ^u, μ^u and λ^l, μ^l are the Lame constants of upper and lower metal layer, respectively.

Appendix B

The nonzero elements of matrix **Q** in Eq. (24) are given by.

$$
\begin{aligned}
Q_{11} &= n^l\left(\lambda^l+2\mu^l\right)+n^u\left(\lambda^u+2\mu^u\right)+c_{11} \\
&\quad +p^2\left(n^l\mu^l+n^u\mu^u+c_{66}\right)-2c^2\left(n^l\rho^l+n^u\rho^u+\rho^m\right), \\
Q_{12} &= p\left(n^l\mu^l+n^u\mu^u+c_{12}+c_{66}\right), \\
Q_{13} &= \xi\left(\lambda^l+2\mu^l\right)\frac{n^l\left(n^l+1\right)}{2}-\xi\left(\lambda^u+2\mu^u\right)\frac{n^u(n^u+1)}{2} \\
&\quad +\xi p^2 n^l\left(n^l+1\right)\mu^l-\xi p^2 n^u\left(n^u+1\right)\mu^u+\xi c^2 n^u\left(n^u+1\right)\rho^u-\xi c^2 n^l\left(n^l+1\right)\rho^l, \\
Q_{21} &= p\left(n^l\mu^l+n^u\mu^u+c_{12}+c_{66}\right), \\
Q_{22} &= p^2 n^l\left(\lambda^l+2\mu^l\right)+p^2 n^u\left(\lambda^u+2\mu^u\right) \\
&\quad +p^2 c_{11}+n^l\mu^l+n^u\mu^u+c_{66}-2c^2\left(n^l\rho^l+n^u\rho^u+\rho^m\right), \\
Q_{23} &= \xi p^3\left(\lambda^l+2\mu^l\right)\frac{n^l\left(n^l+1\right)}{2}-\xi p^3\left(\lambda^u+2\mu^u\right)\frac{n^u(n^u+1)}{2} \\
&\quad +\xi p n^l\left(n^l+1\right)\mu^l-\xi p n^u\left(n^u+1\right)\mu^u+p\xi c^2 n^u\left(n^u+1\right)\rho^u-p\xi c^2 n^l\left(n^l+1\right)\rho^l,
\end{aligned}
$$

$$
\begin{aligned}
Q_{31} = & -\left(\lambda^l + 2\mu^l\right)\frac{n^l\left(n^l+1\right)}{2} + \left(\lambda^u + 2\mu^u\right)\frac{n^u(n^u+1)}{2} \\
& - p^2\mu^l\frac{n^l\left(n^l+1\right)}{2} + p^2\mu^u\frac{n^u(n^u+1)}{2} - 2c^2n^u\left(n^u+1\right)\rho^u - 2c^2n^l\left(n^l+1\right)\rho^l \\
Q_{32} = & -p^3\left(\lambda^l + 2\mu^l\right)\frac{n^l\left(n^l+1\right)}{2} + p^3\left(\lambda^u + 2\mu^u\right)\frac{n^u(n^u+1)}{2} \\
& - p\mu^l\frac{n^l\left(n^l+1\right)}{2} + p\mu^u\frac{n^u(n^u+1)}{2} - pc^2n^u\left(n^u+1\right)\rho^u + pc^2n^l\left(n^l+1\right)\rho^l \\
Q_{33} = & -\xi\left(1+p^4\right)\left(\lambda^l + 2\mu^l\right)\frac{3n^l + 6n^{l2} + 4n^{l3}}{12} \\
& - \xi\left(1+p^4\right)\left(\lambda^u + 2\mu^u\right)\frac{3n^u + 6n^{u2} + 4n^{u3}}{12} - \xi\left(1+p^4\right)\frac{(c_{11}+c_{12})}{12} + \\
& - \xi p^2\mu^l\frac{3n^l + 6n^{l2} + 4n^{l3}}{12} - \xi p^2\mu^u\frac{3n^u + 6n^{u2} + 4n^{u3}}{12} - \xi p^2\frac{c_{66}}{6} \\
& + 2\xi^{-1}c^2\left(n^l\rho^l + n^u\rho^u + \rho^m\right) + \xi\left(c^2 + p^2c^2\right)\rho^l\frac{3n^l + 6n^{l2} + 4n^{l3}}{6} \\
& + \xi\left(c^2 + p^2c^2\right)\rho^u\frac{3n^u + 6n^{u2} + 4n^{u3}}{6} + \xi\left(c^2 + p^2c^2\right)\frac{\rho^m}{6}
\end{aligned}
$$

$$
Q_{34} = -2\xi^{-2}\left(1+p^2\right)\tfrac{e_{31}}{\pi},\ Q_{43} = 2\left(1+p^2\right)\tfrac{e_{31}}{\pi},\ Q_{44} = -\left(1+p^2\right)\tfrac{s_{11}}{2} - \xi^{-2}\pi^2\tfrac{s_{33}}{2}.
$$

References

1. Konenkov, Y.K.: A Rayleigh-type flexural wave. Soviet Phys. Acoust. **6**(1), 122–123 (1960)
2. Lawrie, J.B., Kaplunov, J.: Edge waves and resonance on elastic structures: an overview. Math. Mech. Solids **17**(1), 4–16 (2012)
3. Thurston, R.N., Mckenna, J.: Flexural acoustic waves along the edge of a plate. IEEE Trans. Son. Ultrason. **21**(4), 296–297 (1974)
4. Norris, A.N.: Flexural edge waves. J. Sound Vib. **171**(4), 571–573 (1994)
5. Thompson, I., Abrahams, I.D., Norris, A.N.: On the existence of flexural edge waves on thin orthotropic plates. J. Acoust. Soc. Am. **112**(5), 1756–1765 (2002)
6. Zakharov, D.D., Becker, W.: Rayleigh type bending waves in anisotropic media. J. Sound Vib. **261**(5), 805–818 (2003)
7. Fu, Y.B.: Existence and uniqueness of edge waves in a generally anisotropic elastic plate. Q. J. Mech. Appl. Mech. **56**(4), 605–616 (2003)
8. Liu, G.R., Tani, J., Ohyoshi, T., et al.: Characteristics of surface wave propagation along the edge of an anisotropic laminated semi-infinite plate. Wave Motion **13**(3), 243–251 (1991)
9. Fu, Y.B., Brookes, D.W.: Edge waves in asymmetrically laminated plates. J. Mech. Phys. Solids **54**(1), 1–21 (2006)
10. Lu, P., Chen, H.B., Lee, H.P., et al.: Further studies on edge waves in anisotropic elastic plates. Int. J. Solids Struct. **44**(7–8), 2192–2208 (2007)
11. Lagasse, P.E., Oliner, A.A.: Acoustic flexural mode on a ridge of semi-infinite height. Electron. Lett. **12**(1), 11–13 (1976)
12. Norris, A.N., Krylov, V.V., Abrahams, I.D.: Flexural edge waves and comments on 'A new bending wave solution for the classical plate equation' [J Acoust Soc Am 104: 2220–2222 (1998)]. J. Acoust. Soc. Am. **107**(3), 1781–1784 (2000)
13. Piliposian, G.T., Belubekyan, M.V., Ghazaryan, K.B.: Localized bending waves in a transversely isotropic plate. J. Sound Vib. **329**(17), 3596–3605 (2010)
14. Alzaidi, A.S., Kaplunov, J., Prikazchikova, L.: Elastic bending wave on the edge of a semi-infinite plate reinforced by a strip plate. Math. Mech. Solids **24**(10), 3319–3330 (2019)
15. Nie, G.Q., Dai, B., Liu, J.X., Zhang, L.L.: Bending waves in a semi-infinite piezoelectric plate with edge coated by a metal strip plate. Wave Motion **103**(4), 102731 (2021)
16. Belubekyan, M.V., Ghazaryan, K., Marzocca, P., Cormier, C.: Localized bending waves in a rib-reinforced elastic orthotropic plate. J. Appl. Mech. **74**, 169–171 (2007)
17. Alzaidi, A.S., Kaplunov, J., Prikazchikova, L.: The edge bending wave on a plate reinforced by a beam (L). J. Acoust. Soc. Am. **146**(2), 1061–1064 (2019)
18. Kaplunov, J., Prikazchikov, D.A., Rogerson, G.A., Lashab, M.I.: The edge wave on an elastically supported Kirchhoff plate. J. Acoust. Soc. Am. **136**(4), 1487–1490 (2014)
19. Kaplunov, J., Prikazchikov, D.A., Rogerson, G.A.: Edge bending wave on a thin elastic plate resting on a Winkler foundation. Proc. R. Soc. A Math. Phys. Eng. Sci. **472**, 20160178 (2016)
20. Althobaiti, S.N., Nikonov, A., Prikazchikov, D.: Explicit model for bending edge wave on an elastic orthotropic plate supported by the Winkler–Fuss foundation. J. Mech. Mater. Struct. **16**(4), 543–554 (2021)
21. Althobaiti, S., Hawwa, M.A.: Flexural edge waves in a thick piezoelectric film resting on a Winkler foundation. Crystals **12**, 640 (2022)

22. Kaplunov, J., Nobili, A.: The edge waves on a Kirchhoff plate bilaterally supported by a two-parameter elastic foundation. J. Sound Vib. **23**(12), 2014–2022 (2017)
23. Abrahams, I.D., Norris, A.N.: On the Existence of flexural edge waves on submerged elastic plates. Proc. R. Soc. A Math. Phys. Eng. Sci. **456**, 1559–1582 (2000)
24. Kaplunov, J., Prikazchikova, L., Alkinidri, M.: Antiplane shear of an asymmetric sandwich plate. Continuum Mech. Thermodyn. **33**, 1247–1262 (2021)
25. Wilde, M.V., Surova, M.Y., Sergeeva, N.V.: Asymptotically correct boundary conditions for the higher-order theory of plate bending. Math. Mech. Solids **27**(9), 1813–1854 (2022)
26. Piliposian, G.T., Ghazaryan, K.B.: Localized bending vibrations of piezoelectric plates. Waves Random Complex Med. **21**(3), 418–433 (2011)
27. Nie, G.Q., Lei, Z.Y., Liu, J.X., Zhang, L.L.: Bending waves localized along the edge of a semi-infinite piezoelectric plate with orthogonal symmetry. Front. Mater. **9**, 1031538 (2022)
28. Carrera, E.: Historical review of zig-zag theories for multilayered plates and shells. Appl. Mech. Rev. **56**(3), 287–308 (2003)
29. Kapuria, S., Nath, J.K.: Coupled global-local and zigzag-local laminate theories for dynamic analysis of piezoelectric laminated plates. J. Sound Vib. **332**, 306–325 (2013)
30. Ye, R.C., Tian, A.L., Chen, Y.M., et al.: Sound transmission characteristics of a composite sandwich plate using multi-layer first-order zigzag theory. Thin-Walled Struct. **179**, 109607 (2022)
31. Keshtegar, B., Motezaker, M., Kolahchi, R., et al.: Wave propagation and vibration responses in porous smart nanocomposite sandwich beam resting on Kerr foundation considering structural damping. Thin-Walled Struct. **154**, 106820 (2020)
32. Nath, J.K., Mishra, B.B., Das, T.: Improved electromechanical response in laminated piezoelectric plates using a zigzag theory. J. Aerosp. Eng. **34**(6), 04021083 (2021)
33. Quek, S.T., Wang, Q.: On dispersion relations in piezoelectric coupled-plate structures. Smart Mater. Struct. **9**(6), 859–867 (2000)
34. Ke, L.L., Liu, C., Wang, Y.S.: Free vibration of nonlocal piezoelectric nanoplates under various boundary conditions. Physica E **66**, 93–106 (2015)
35. Reddy, J.N.: Energy Principles and Variational Methods in Applied Mechanics. Wiley, Hoboken (2017)
36. Luan, G.D., Zhang, J.D., Wang, R.Q.: Piezoelectric Transducer and Arrays (revised edition) (in Chinese). Peking University Press, Beijing (2005)
37. Rose, J.L.: Ultrasonic Waves in Solid Media. Cambridge University Press, Cambridge (1999)